Supplementary methods

Surgical procedure for IRI

2% isoflurane inhalation was used as anesthesia, and mice were then fixed on a heating blanket (37 ℃). After opening the abdominal cavity via midline incision, a micro-aneurysm clip was placed on the left renal pedicle. Complete ischemia was indicated by color change of the kidney from red to dark purple. After 30 minutes, the micro-aneurysm clip was released, and the right kidney was removed.

Flow cytometry

Mouse bone marrow was collected on WT (C57BL/6) and Caspase $3^{-/-}$ mice as described. Single-cells suspensions were then immediately stained for flow cytometry.[1] All of the experiments were performed on BD LSRII flow cytometer (Becton Dickinson, San Jose, CA, USA). Viable cells were gated using Live/dead Fixable aqua dead cell stain kit (Aquavid) (Molecular probes, Eugene, OR, USA), CD34+ CD45+ progenitor cells were determined by using anti-mouse CD34-BV421 (BD Bioscience, San Jose, CA, USA) and anti-mouse CD45-APC (BD Bioscience, San Jose, CA, USA). All data were analyzed with FlowJo software 10.0 (Ashland, OR, USA). Results were expressed as the percentage of CD34+CD45+ cells among viable bone marrow cells.

Electron Microscopy Examination

Renal tissue was cut into small pieces that were fixed with 3% glutaraldehyde, post-fixed with 1% osmium tetroxide, and incubated consecutively in an ascending acetone series (50%, 70%, and 90%), with a final incubation in 100% ethanol for hydration. After incubation in

acetone, the tissue was embedded in Epon. 1-nm sections were cut and stained using uranyl acetate and lead citrate. Electron microscopy images were taken with the Phillips EM208 electron microscope.

K1 medium

K1 medium is constituted with following products [Dulbecco's modified Eagle's medium (DMEM): Hams F12] (50:50) (Invitrogen-Gibco, Carlsbad, CA, USA), 5% fetal bovine serum (Invitrogen, Waltham, USA), hormone mix [5 μg/mL insulin, 1.25 ng/mL prostaglandin E1, 34 pg/mL triiodothyronine, 5 μg/mL transferrin, 1.73 ng/mL sodium selenite and 18 ng/mL of hydrocortisone] and 25 ng/mL epidermal growth factor.

Supplementary reference

1. Madaan, A, Verma, R, Singh, AT, Jain, SK, Jaggi, M: A stepwise procedure for isolation of murine bone marrow and generation of dendritic cells. *2014*, 2014.

Supplementary figure legends

Supplementary Figure 1a: Caspase-3 deficiency aggravates IRI-induced tubular injury. A) Representative H&E–stained murine renal cortical sections at baseline (N ≥ 3 per group; magnification 200X). Bar scale = 50μm. B) Urinary levels of cystatin C in wild-type and caspase-$3^{-/-}$ mice at baseline and at days 1, 2, 3, 7 or 21 post-IRI. C) Representative KIM-1 immunohistochemistry in renal cortical sections from wild-type and caspase-$3^{-/-}$ mice at baseline (N ≥ 3 per group; magnification 200X). Bar scale = 50μm. Values are mean ± SEM.*$P < 0.05$ compared between WT and KO at the same time point.

Supplementary Figure 1b: D) Left panels: representative images of CD45 immunohistochemistry in renal cortical sections from wild-type and caspase-3$^{-/-}$ days 1 and 7 post-IRI. Bar scale = 50µm (magnification 200X). Right panels: quantification of CD45 in murine renal cortical sections at baseline and 1, 2, 3, 7 or 21 days post-IRI. E) Left panel: representative images of vascular cell adhesion molecule-1 (VCAM-1) immunohistochemistry in renal cortical sections from wild-type and caspase-3$^{-/-}$ mice at baseline and 3 or 21 days post-IRI. Bar scale = 50µm (magnification 200X). Right panels: quantification of VCAM-1 immunohistochemistry. Values are mean ± SEM.*$P < 0.05$, compared between WT and KO at the same time point.

Supplementary Figure 2: Caspase-3 deficiency increases IRI-induced necroptosis in tubular cells. A) Representative H&E-stained murine renal cortical sections 1 day post-IRI in wild-type and caspase-3-/- mice (magnification 400X). Bar scale = 50µm. B) Representative RIPK3 immunohistochemistry in renal cortical sections from wild-type and caspase-3$^{-/-}$ mice at baseline (magnification 200X).

Supplementary Figure 3: A) Left panel: representative images of CD34 immunohistochemistry in renal cortical sections from wild-type and caspase-3$^{-/-}$ mice at day 1 post-IRI (magnification 200X). Right panels: quantification of CD34 in murine renal cortical sections at 1, 2, 3 or 7 days post-IRI. Bar scale = 50µm. B) Left panel: quantification of CD34+/CD45+ bone marrow derived cells in wild-type and caspase-3$^{-/-}$ mice at baseline. Right panels: representative FACs scatter plots for CD34+/CD45+ bone marrow derived cells. C) Representative image of

MECA-32 immunohistochemistry in renal cortical sections from wild-type and caspase-3$^{-/-}$ mice at baseline (magnification 200X). Values are mean ± SEM.*P < 0.05, compared between WT and KO at the same time point.

Supplementary Figure 4: A) Representative α-SMA immunohistochemistry in murine renal cortical sections at baseline (N ≥ 3 per group). Bar scale = 50μm. B) Left panel: representative western blot images of α-SMA 3 days post-IRI (N ≥ 6 per group). Right panel: quantification α-SMA western blot 3 days post-IRI. C) Representative images of Sirius Red staining at renal cortical medullary junction sections from wild-type and caspase-3$^{-/-}$ mice at baseline (N ≥ 3 per group; magnification 200X). Bar scale = 50μm. Values are mean ± SEM.*P < 0.05, compared between WT and KO at the same time point.

Supplementary Figure 5: Caspase-3 deficiency attenuates IRI-induced microvascular rarefaction. A) Quantification of MECA-32 staining in murine renal cortical sections from wild-type and caspase-3-/- mice at baseline and 1, 2, 3, 7 or 21 days post-IRI. B) Quantification of α-SMA staining in PTC in murine renal cortical sections from wild-type and caspase-3$^{-/-}$ mice at baseline and at 1, 2, 3, 7 or 21 days post-IRI. C) Upper panel: representative images of glomerular α-SMA staining in wild-type and caspase-3$^{-/-}$ at baseline and 1, 2, 3, 7 or 21 days after IRI (magnification 200X). Bar scale = 50μm. Lower panel: Quantification of glomerular α-SMA staining in murine renal cortical sections from wild-type and caspase-3$^{-/-}$ mice at baseline and 1, 2, 3, 7 or 21 days post-IRI. Values are mean ± SEM.*P < 0.05, compared between WT and KO at the same time point.

Supplementary Figure 6: Upper panels: representative images of activated caspase-3 immunohistochemistry in renal cortical sections from wild-type and caspase-$3^{-/-}$ mice at baseline and 1, 2, 3, 7 or 21 days after IRI (magnification 200X). Bar scale = 50μm. Lower panel: quantification of activated caspase-3 staining in murine renal cortical sections from wild-type and caspase-$3^{-/-}$ mice at baseline and 1, 2, 3, 7 or 21 days post-IRI. Values are mean ± SEM. ***$P < 0.001$, compared between baseline (pre) and other time points.

Supplementary Figure 7: A) Representative image of HIF-1α staining in murine renal cortical sections from wild-type and caspase-$3^{-/-}$ mice that were sacrificed pre-operation ($N \geq 3$ per group; magnification 200X). Bar scale = 50μm B) Serum creatinine levels in wild-type and caspase-$3^{-/-}$ mice at baseline or at 1, 2, 3, 7 or 21 days post-IRI or sham treatment. C) Mean tubular injury scores of ten randomly chosen high-power fields in H&E-stained renal cortical sections from wild-type and caspase-$3^{-/-}$ mice at baseline and at 1, 2, 3, 7 or 21 days post-IRI. D) Quantification of rouleaux formation in H&E-stained renal cortical sections from wild-type and caspase-$3^{-/-}$ mice at baseline and at 1, 2, 3, 7 or 21 days post-IRI. Values are mean ± SEM.*$P < 0.05$, compared between WT and KO at the same time point.

Supplementary Figure 8: A) Serum creatinine levels in wild-type and caspase-$3^{-/-}$ mice treated with the pan-caspase inhibitor Z-VAD-FMK or vehicle (DMSO) and sacrificed 1 day post-IRI or sham treatment. Values are mean ± SEM.*$P < 0.05$.

A HE staining pre

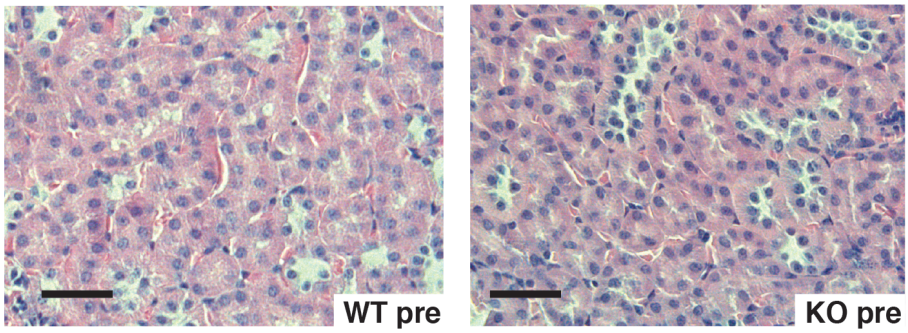

B Uriary Cystatin C

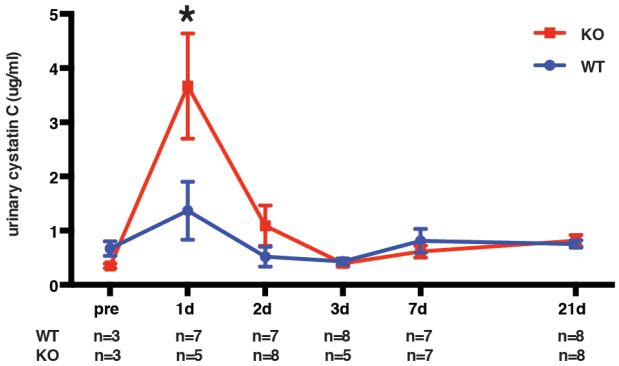

C KIM-1 IHC pre

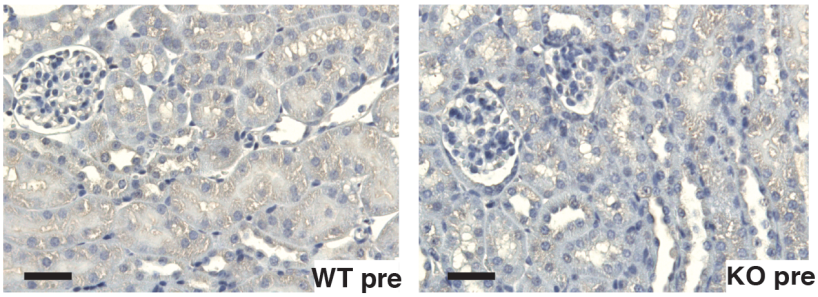

Figure S1a: Caspase-3 deficiency aggravates IRI-induced tubular injury.

D CD45 IHC

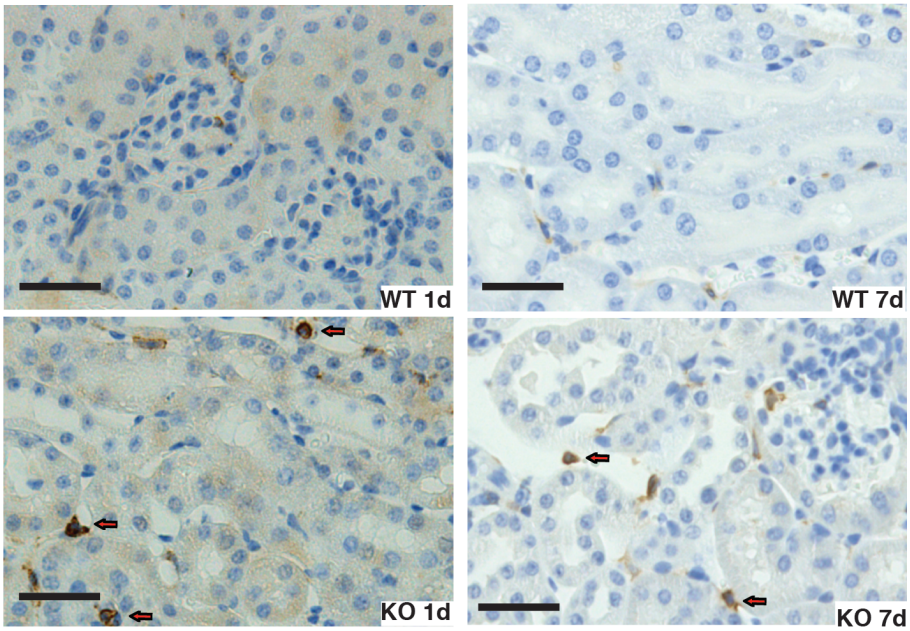

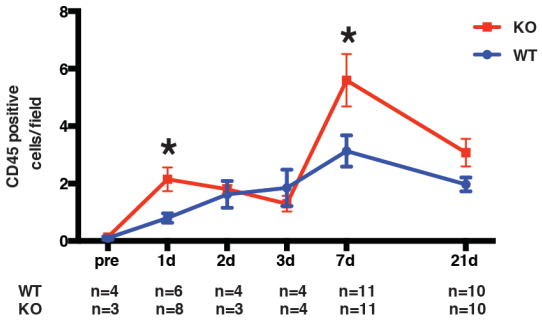

E VCAM-1 IHC

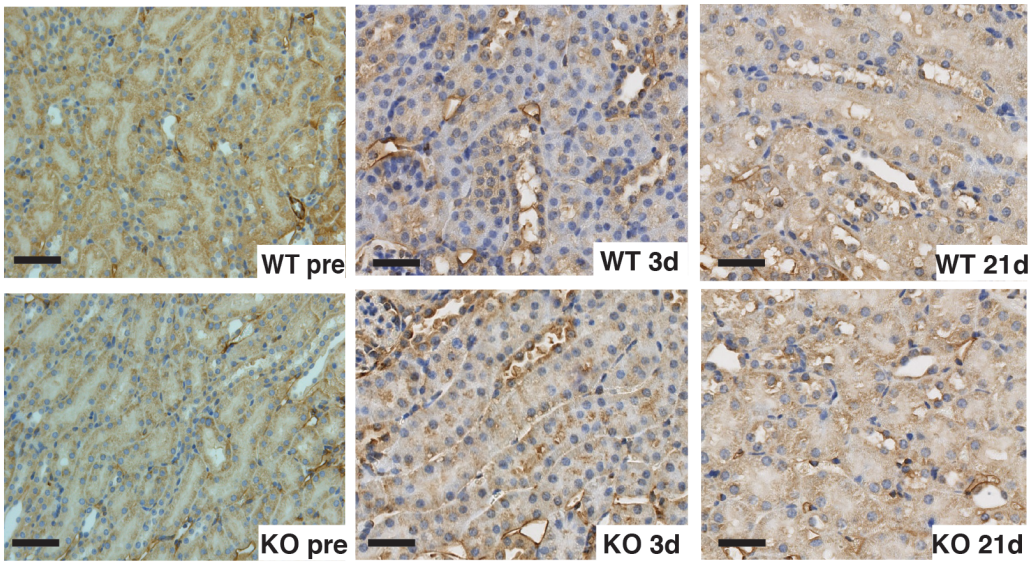

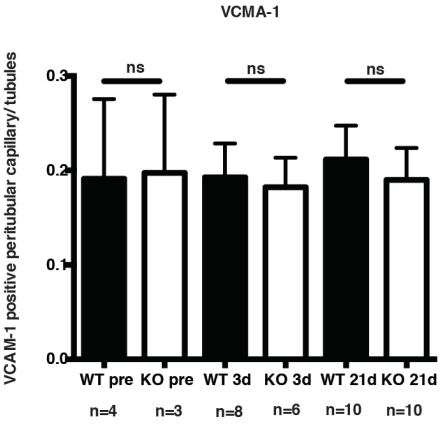

Figure S1b: Caspase-3 deficiency aggravates IRI-induced tubular injury.

A HE

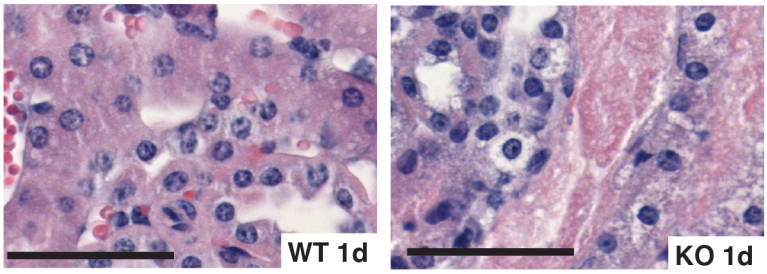

B RIPK3 IHC pre

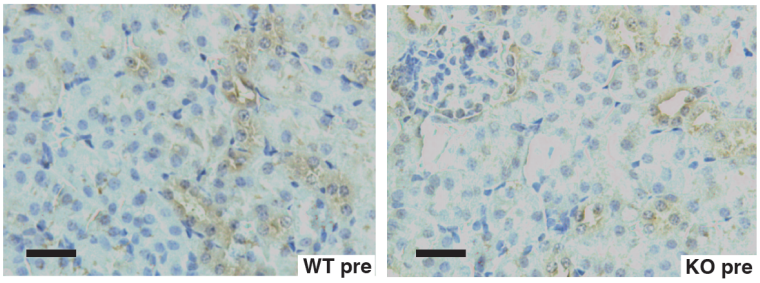

Figure S2: Caspase-3 deficiency increases IRI-induced necroptosis in tubular cells.

A CD34 IHC

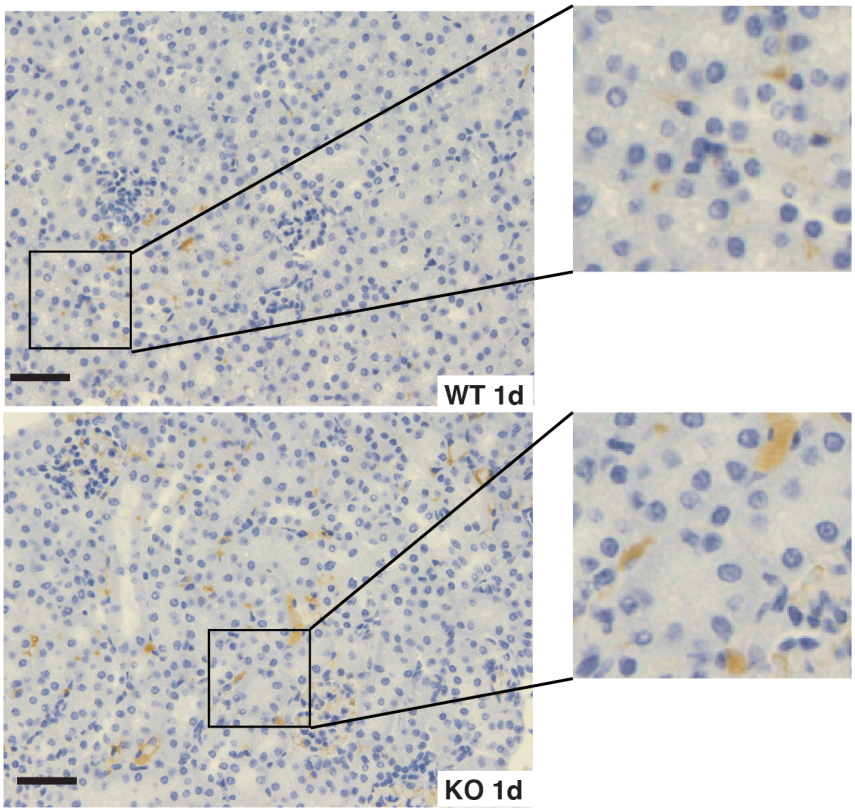

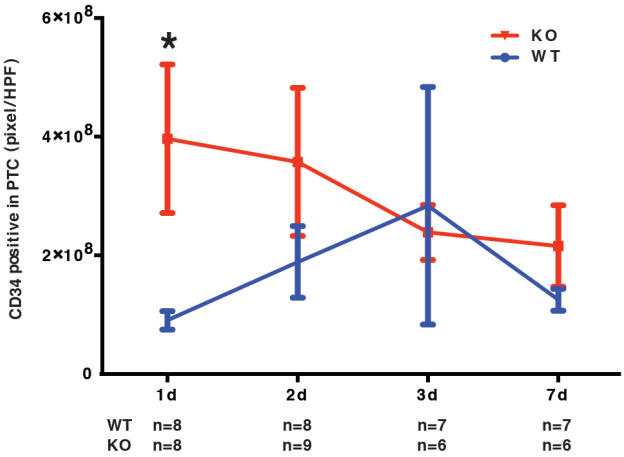

B Percentage of CD34+/CD45+ cells in bone marrow derived cells(female)

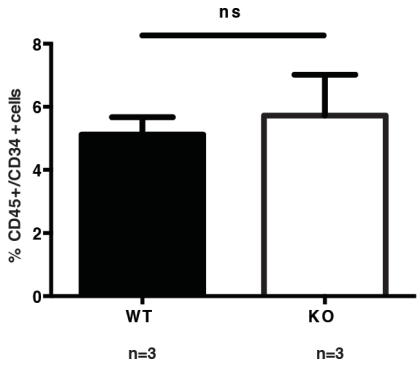

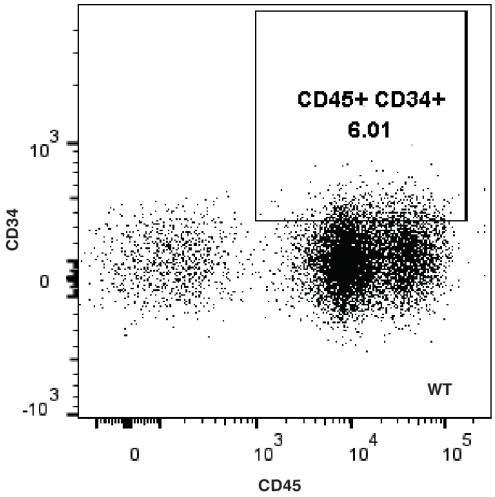

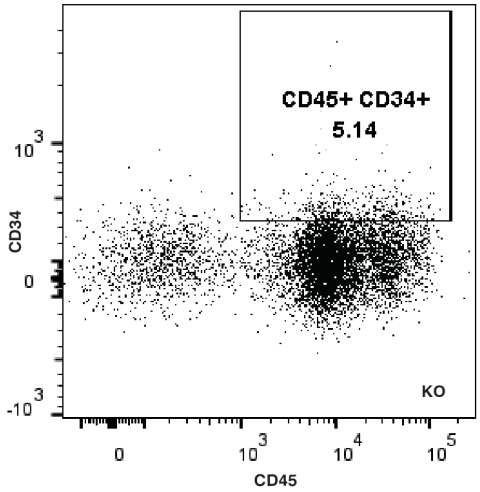

C MECA-32 IHC pre

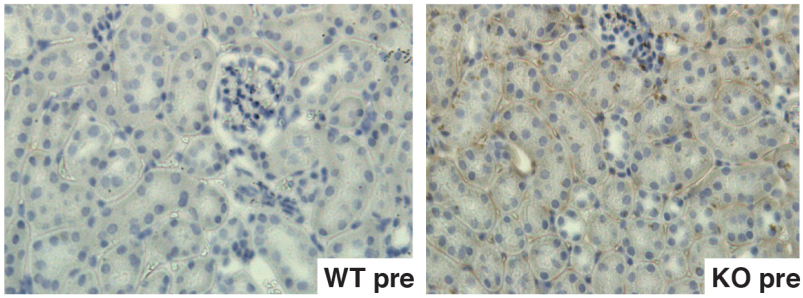

Figure S3: Caspase-3 deficiency benefits endothelial cells preservation after IRI.

A α-SMA IHC pre

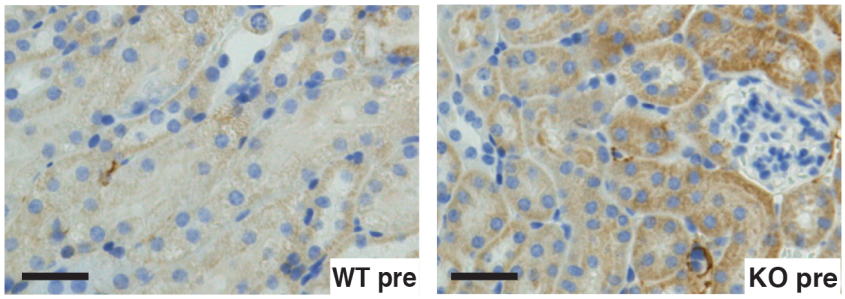

B α-SMA WB 3d

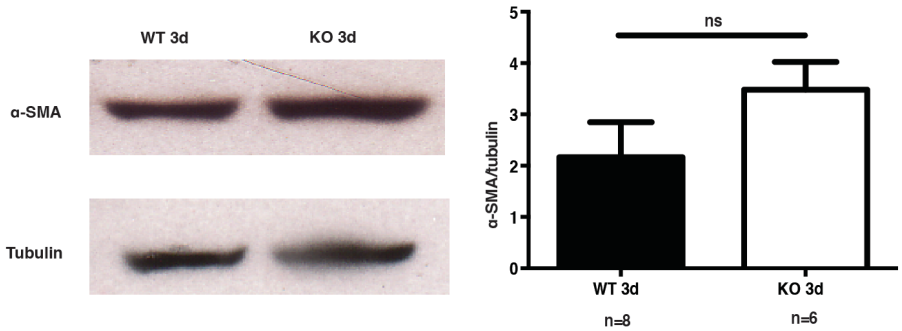

C Sirius Red staining pre

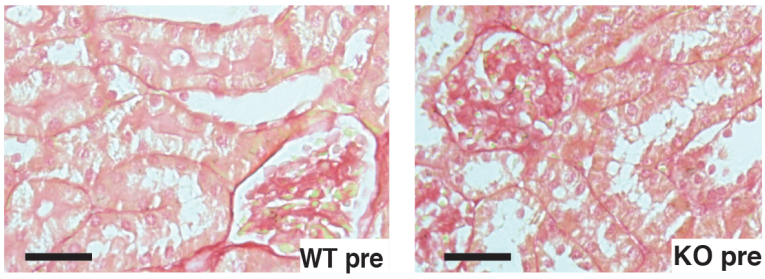

Figure S4: Caspase-3 deficiency attenuates IRI-induced upregulation of pro-fibrotic markers.

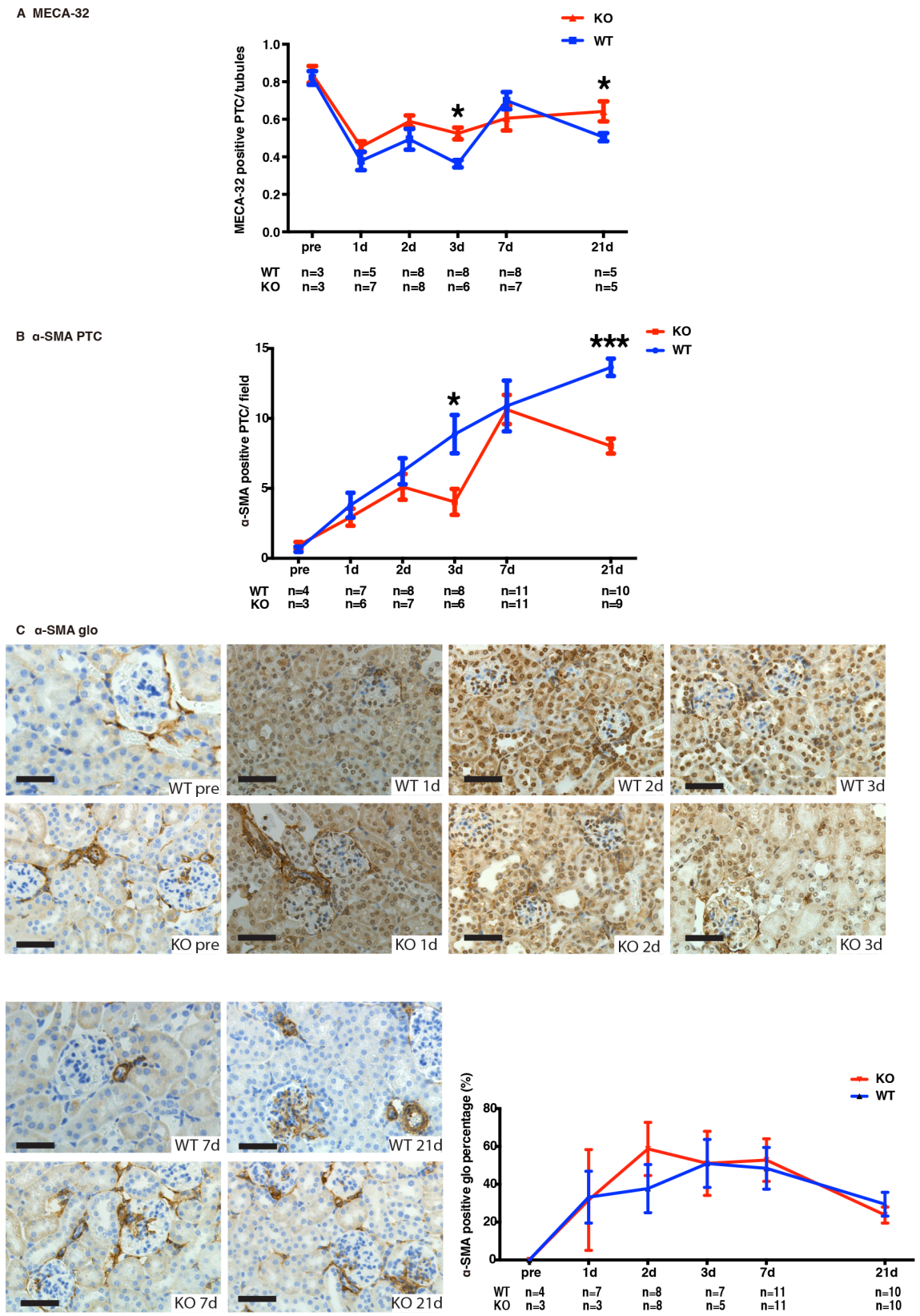

Figure S5: Caspase-3 deficiency attenuates IRI-induced microvascular rarefaction.

caspase-3 IHC

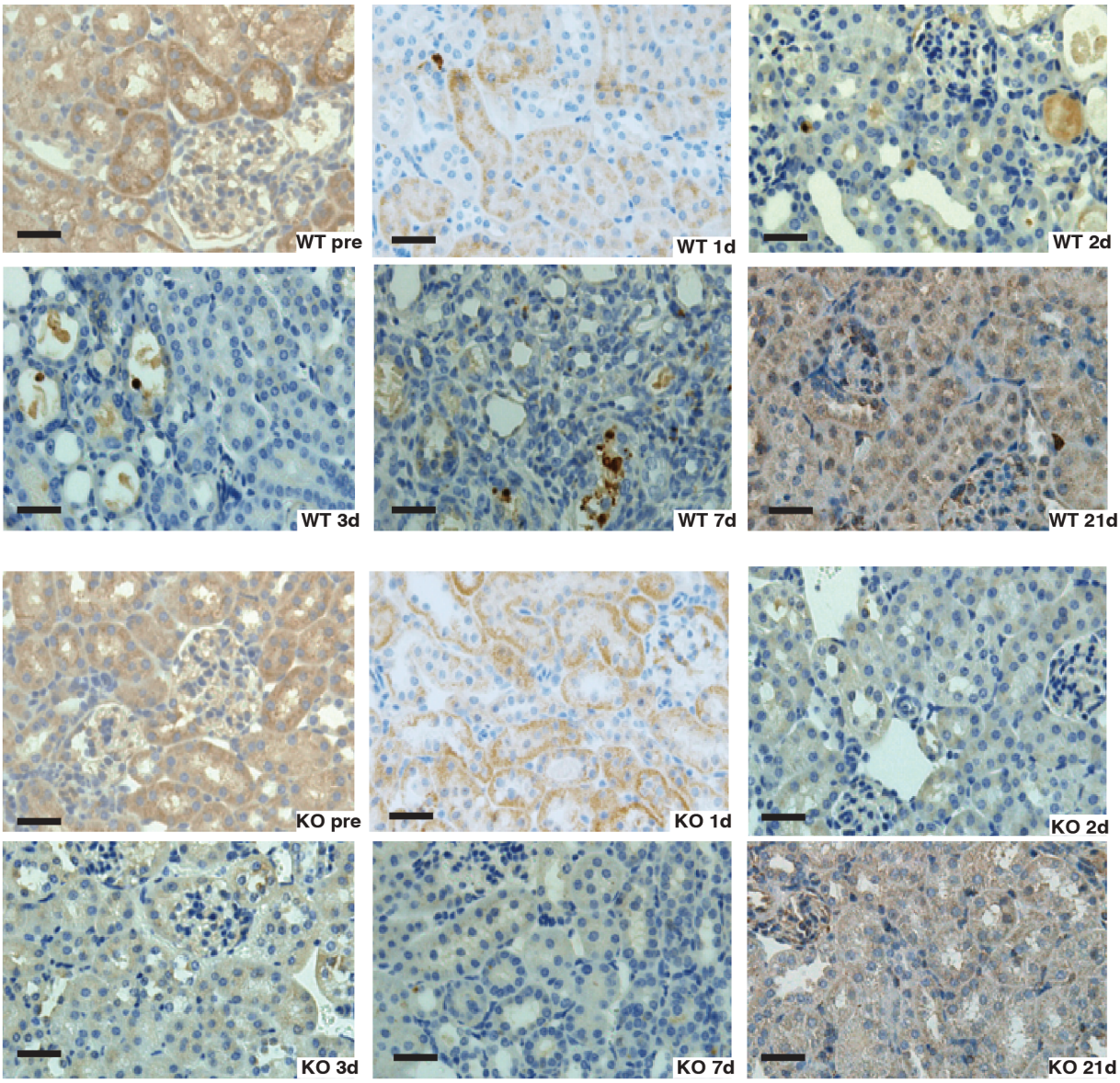

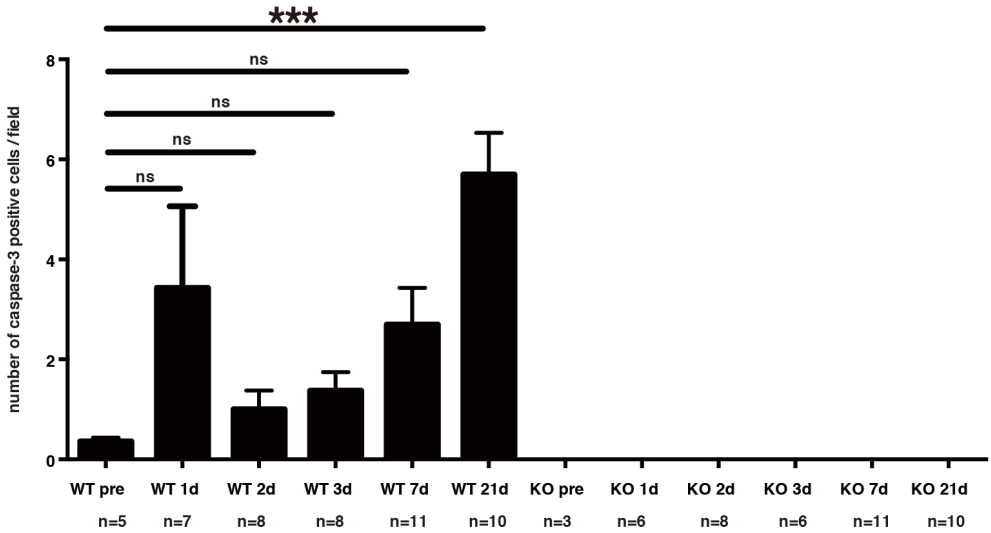

Figure S6: Caspase-3 activation post ischemia-reperfusion Injury.

A HIF-1α IHC pre

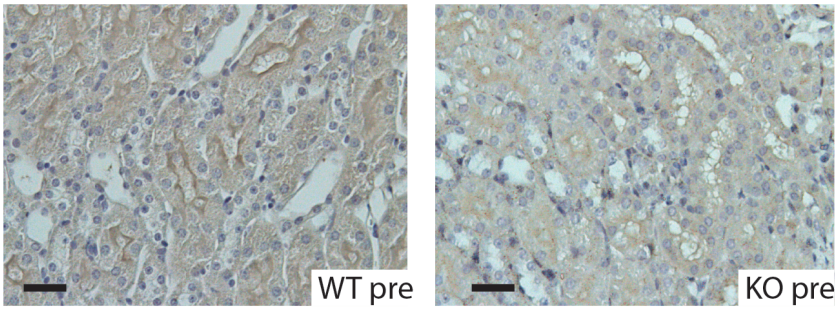

B Serum creatinine level

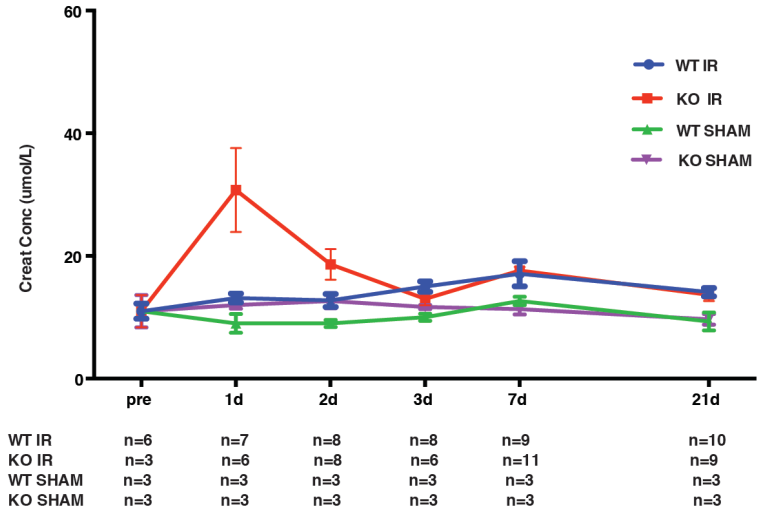

C Tubular injury score

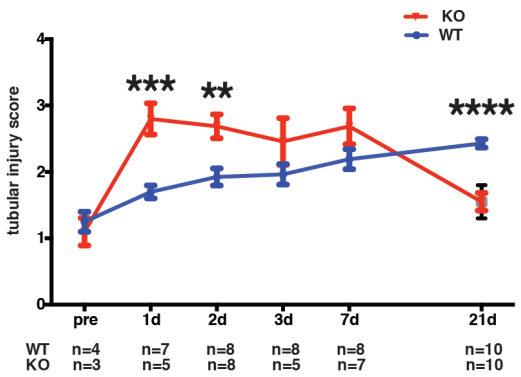

D Rouleaux Formation

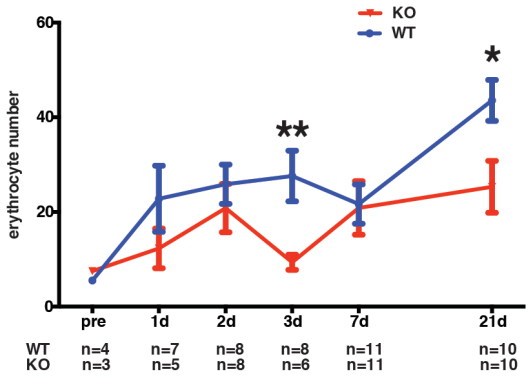

Figure S7: Caspase-3 deficiency prevents IRI-induced long-term renal dysfunction.

Serum creatinine levels

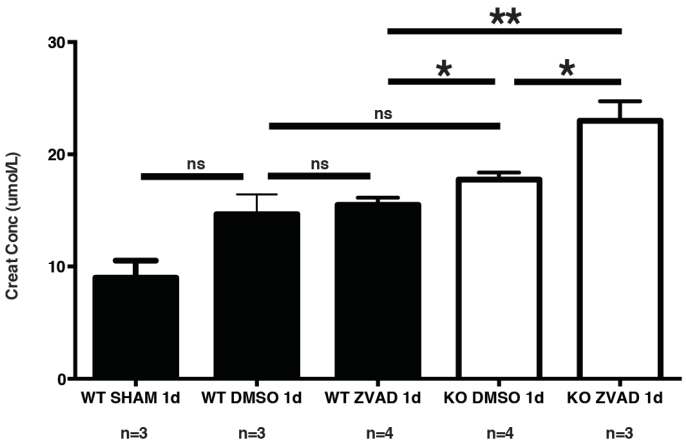

Figure S8: Pan-caspase inhibition further aggravates IRI induced renal dysfunction.